

Research Article

Anisotropic Ferro- and Dielectric Properties of Textured $\text{Bi}_4\text{Ti}_3\text{O}_{12}$ Ceramics Prepared by the Solid-State Reaction Based on Multiple Calcination

Xiangyu Mao, Wei Wang, Hui Sun, and Xiaobing Chen

College of Physics Science and Technology, Yangzhou University, Yangzhou 225002, China

Correspondence should be addressed to Xiaobing Chen, xbchen@yzu.edu.cn

Received 3 July 2010; Revised 22 September 2010; Accepted 13 October 2010

Academic Editor: Z. H. Barber

Copyright © 2010 Xiangyu Mao et al. This is an open access article distributed under the Creative Commons Attribution License, which permits unrestricted use, distribution, and reproduction in any medium, provided the original work is properly cited.

The grain-oriented $\text{Bi}_4\text{Ti}_3\text{O}_{12}$ (BIT) samples were prepared by the solid-state reaction method with a multicalcination process. The grain-oriented BIT samples exhibit anisotropic structural, ferroelectric, piezoelectric, and dielectric properties. The remanent polarization ($2P_r$) and the piezoelectric constant (d_{33}) of *a/b*- and *c*-direction BIT ceramics are $49.5 \mu\text{C cm}^{-2}$, 22.2 pC N^{-1} and $6.7 \mu\text{C cm}^{-2}$, 6.9 pC N^{-1} , respectively. The dielectric anomalies of samples are observed around 157 K and 232 K. The dielectric anomalies at around 157 K are related to oxygen vacancies. The activation energy of the dielectric relaxation of this anomaly is estimated to be 1.36 eV. Another dielectric anomaly at around 232 K is related to polarizable domains and the viscous motion of domain walls.

1. Introduction

The layered bismuth compounds first studied by Aurivillius are known to possess a structure expressed by the general formula $(\text{Bi}_2\text{O}_2)^{2+}(\text{A}_{m-1}\text{B}_m\text{O}_{3m+1})^{2-}$, where A is a mono-, di-, or trivalent ion allowing dodecahedral coordination, B is a transition element suited to octahedral coordination, and *m* is an integer which represents the number of BO_6 octahedron in $(\text{A}_{m-1}\text{B}_m\text{O}_{3m+1})^{2-}$ between the $(\text{Bi}_2\text{O}_2)^{2+}$ [1]. The crystal structure of $\text{Bi}_4\text{Ti}_3\text{O}_{12}$ (BIT), *m* = 3, is monoclinic with β very close to 90° [2]. Investigation of BIT single crystal revealed that its Curie temperature is 676°C and spontaneous polarizations (P_s) along *a* and *c* axes are $50 \pm 5 \mu\text{C/cm}^2$ and $4 \pm 0.1 \mu\text{C/cm}$, respectively [3, 4]. BIT has various applications in the electric industry, including capacitors, transducers, memory devices, and sensors [5–7]. The usefulness of certain piezoelectric ceramics in sensing and actuating devices can be enhanced by means of grain orientation or texture construction. Texture in polycrystalline materials refers to the mutual orientation of the crystallographic lattices of individual grains. However, the layered structure and low crystal symmetry of BIT lead to difficulty in polarizing conventional polycrystalline BIT ceramics [8]. It is desirable to obtain BIT ceramics

having grain orientation or textured microstructures because improved properties can be achieved in grain-oriented ceramics more than that have a random-oriented grain structure [9–11]. Mechanical force is normally applied to prepare grain-oriented ceramics, that is, hot-forging (HF), hot-pressing (HP), templated grain growth (TGG), and tape-casting processes (TCPs).

The dielectric properties of ferroelectric materials are closely related to crystal structure and oxygen vacancies, which can be controlled by doping or annealing in different oxygen partial pressure conditions. After the investigation of the dielectric characteristics of BIT single crystal [4], there have been several reports on the dielectric anomalies of these materials, such as that observed around 250°C [12–14], which has been attributed to an oxygen-ion-jump-related relaxation process and 90° domain walls, that was observed around 400°C in BIT ceramics [5]. It seems that BIT exhibits complex dielectric behavior; however, detailed information of the low-temperature dielectric characteristics in grain-oriented $\text{Bi}_4\text{Ti}_3\text{O}_{12}$ ceramics has not been reported so far.

In the present work, we synthesized the grain-oriented BIT ceramics and reported their room temperature ferroelectric behavior and low-temperature dielectric properties from 140 K to 300 K.

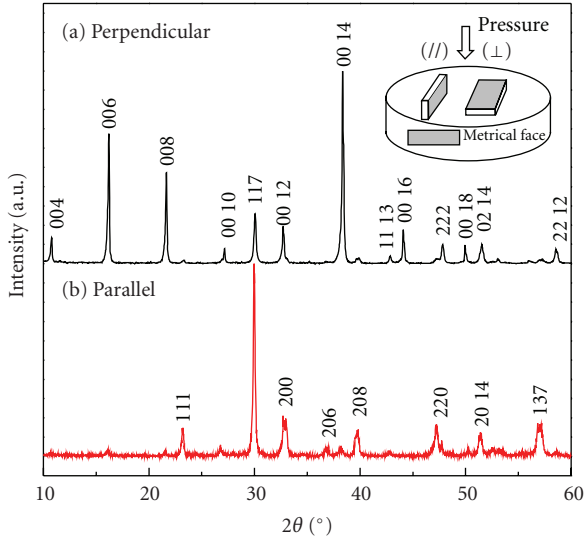


FIGURE 1: XRD patterns of the grain-oriented BIT ceramics (a) perpendicular, (b) parallel to the press direction and inset: sketch of samples preparation. Samples were cut from the cylindrical samples along the directions parallel and perpendicular to the pressing direction.

2. Experimental Procedure

BIT samples were prepared by the solid-state reaction method with multiple intermediate calcination process. The starting materials of Bi_2O_3 (analytic pure) and TiO_2 (spectral pure) powders in stoichiometry were finely ground (15 wt% excess of Bi_2O_3 were added to compensate for the volatilization of Bi_2O_3 in the sintering process), there powders were mixed thoroughly and ground in anhydrous alcohol by ball mill for 24 h ($n = \sim 420$ N/min). Mixed powders were firstly dried at 110°C in oven and then pressed into pellets and calcined at 760°C for 8 h. The sintered pellets were pulverized in the same manner and undergo two calcinations procedure at 780°C for 16 h, and 800°C for 24 h, respectively. The powders were finally pressed into cylindrical samples ($\Phi 80$ mm) and sintered at 1140°C for 16 h.

To investigate the microstructure and electrical properties, samples were obtained by slicing from the cylindrical samples along ($//$) and perpendicular (\perp) the axis of cylinder, as shown schematically in the inset of Figure 1. The crystal structure and grain orientation of samples were examined based on intensities of XRD peaks. The microstructures of samples were observed using SEM (Philips, XL 30 ESEM). The ferroelectric properties were measured using a Precision LC ferroelectric analyzer (Radiant Technology product). Both real permittivity (ϵ) and dielectric loss of samples as functions of temperature ranging from 140 K to 300 K with the heating rate of $0.5^\circ\text{C}/\text{min}$ were obtained with broadband dielectric spectrometer (Novocontrol Technologies, Germany). In order to compare the dielectric behavior, some samples were annealed in an oxidizing atmosphere or poled in silicon oil at 180°C for 2 min under dc electric field of 20 kV/cm.

3. Results and Discussion

Figure 1 shows the XRD patterns of BIT ceramics for the surfaces parallel and perpendicular to the cylinder axis. The XRD pattern of the samples of BIT shows a single phase of Aurivillius phase with $m = 3$. The intensity of $(00l)$ peaks of XRD with perpendicular (\perp) samples was strong with (0014) peak the most. Nevertheless, the pattern of the parallel ($//$) sample appears to be a stronger (117) peak, and the $(00l)$ peaks disappear or become very weak. The XRD patterns of all the parallel and perpendicular samples are much different from random-oriented grain structure [15], which exhibit grain-oriented ceramics of the BIT samples.

Figures 2(a) and 2(b) show SEM micrographs of the surface perpendicular and parallel to the cylinder axis. These micrographs show a grain-oriented BIT ceramics. The plate-like BIT grains are aligned in the high order along their planar direction. The perpendicular (\perp) and parallel ($//$) sample were c - and a/b -direction BIT ceramics [16]. We sintered our samples under ambient pressure which could avoid using high-pressure sintering. It is considered that the multicalcination process facilitates the grain growth along the direction having lower interfacial energy, which is conducive to the grain-oriented dynamics.

Figure 3 shows the Polarization-Electrical hysteresis loops of the grain-oriented samples recorded at room temperature. The loops are strongly anisotropic, with much higher remnant polarization, $2P_r$, [$//$] sample than [\perp] sample the $2P_r$ values of [$//$] and [\perp] samples are $49.5 \mu\text{C cm}^{-2}$ and $6.7 \mu\text{C cm}^{-2}$, respectively. There is no large $2P_r$ in [\perp] samples with orientation close to c -axis. This is same to the results reported for BIT thin films and the textured BIT ceramics. Form the viewpoint of crystal structure, tetragonal and monoclinic groups naturally allow a c -axis major P_r component, whereas the orthorhombic $B2cb$ only allows an a -axis major polarization [17]. After being polarized at 180°C for 2 min using a dc field of 20 kV cm^{-1} , the sample of parallel ($//$) direction exhibits a higher d_{33} -value (22.2 pC N^{-1}), and the perpendicular (\perp) sample was only 6.9 pC N^{-1} . This is consistent with the value in these samples. The grain-oriented samples of BIT exhibit anisotropy properties with ferroelectric and piezoelectric properties, the ferroelectric and piezoelectric properties of a/b grain-oriented samples direction samples were better than c grain-oriented BIT ceramics; however, the ratios of $2P_{r(//)} : 2P_{r(\perp)}$ and $d_{33(//)} : d_{33(\perp)}$ were about 7.3 and only 3.2, so the anisotropic piezoelectric properties were not as obvious as that in ferroelectric natures.

The temperature dependence of dielectric constants (ϵ) of the samples at various frequencies ($1.139 \sim 498.8$ kHz) exhibits the anisotropic microstructure shown in Figures 4(a) and 4(b). The dielectric constants of two directions samples were increased with an increase of the measured temperature, and the dielectric anomalies of both the samples observed around 157 K and 232 K. The dielectric constants of the perpendicular-cut samples are lower than that parallel to the counterpart. At the room temperature at frequencies 1.139 kHz, the value of the dielectric constants with [\perp] and [$//$] samples was about 91 and 195, respectively.

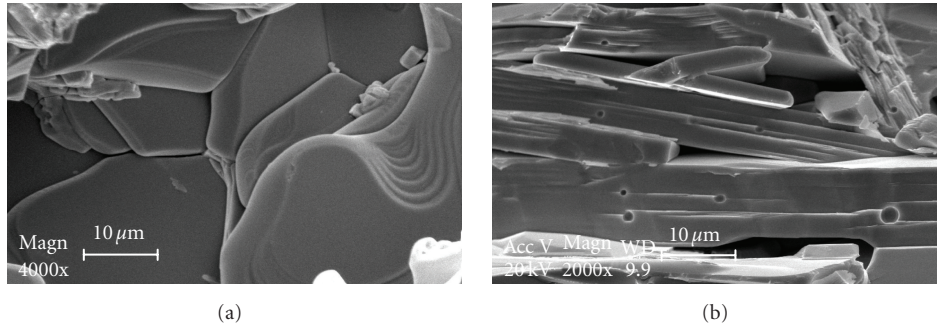


FIGURE 2: SEM images of grain-oriented BIT ceramics (a) perpendicular and (b) parallel to the press direction.

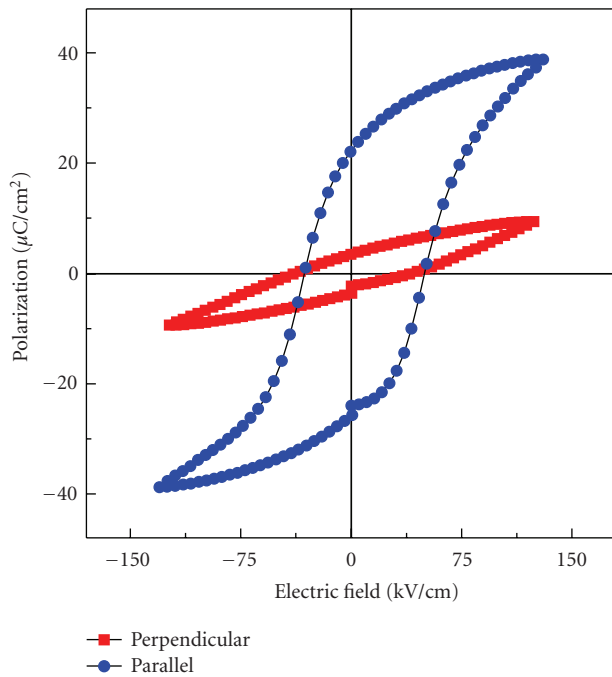


FIGURE 3: The ferroelectric-polarization hysteresis loops showing polarization versus electric field.

The inset of Figure 4 shows the DSC curve. The “similar” phase transition was detected at ~ 209 K. The anomalies of the temperature dependence of dielectric constants at ~ 232 K may be related to the inflexion in DSC curve. However, the phase transition studies of single crystal and ceramics of BIT over a wide temperature range showed only one phase transition at Curie temperature (948 K) [3, 18]. From 15 K to 300 K, the phase of BIT was normal ferroelectrics [19], and the crystal structure was the orthorhombic lattice [20]. The mechanism for its occurrence at DSC curve and the two dielectric anomalies are still under further investigation.

The temperature dependence of the dielectric loss ($\tan \delta$) of specimens at different frequencies (1.139 \sim 498.8 kHz) is shown in Figures 5(a)–5(c) and 5(d)–5(f). The dielectric loss data exhibit anisotropy properties (shown in Figures 5(a) and 5(d)); the value of $\tan \delta$ of $[\perp]$ sample was lower

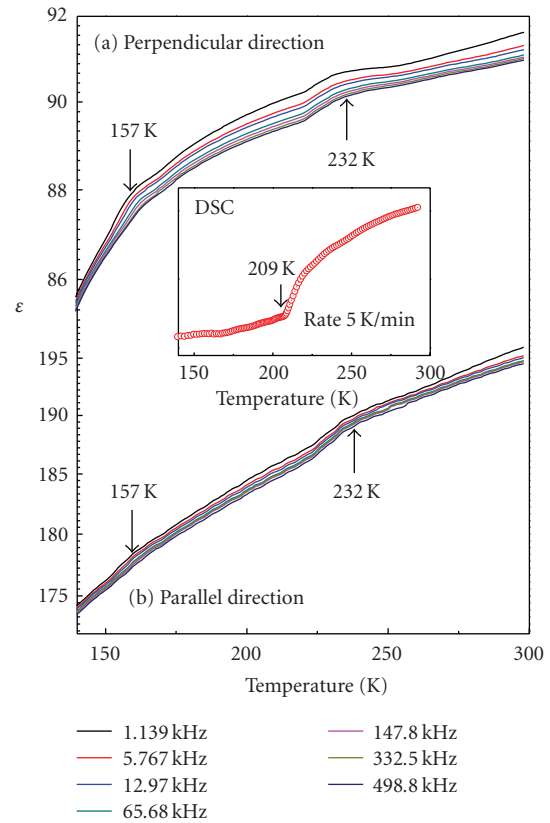


FIGURE 4: The temperature dependence of dielectric constants, (a) perpendicular direction; (b) parallel direction inset: DSC curve measured of BIT sample on heating.

than that of $[\parallel]$ sample. The temperature dependence of dielectric loss of perpendicular (\perp) and parallel (\parallel) samples showed two dielectric loss peaks, one is at ~ 155 K for both cases, and the other is at 223 K (\perp sample) and 214 K (\parallel sample), respectively. The lower temperature peak at ~ 155 K; the peak shifts to higher temperature with the increase of the frequency and exhibits relaxation characteristic (marked in inset of Figures 5(a) and 5(d)). From the slope of $\ln f - 1000/T$, the activation energy (H) can be obtained, which is 1.36 eV.

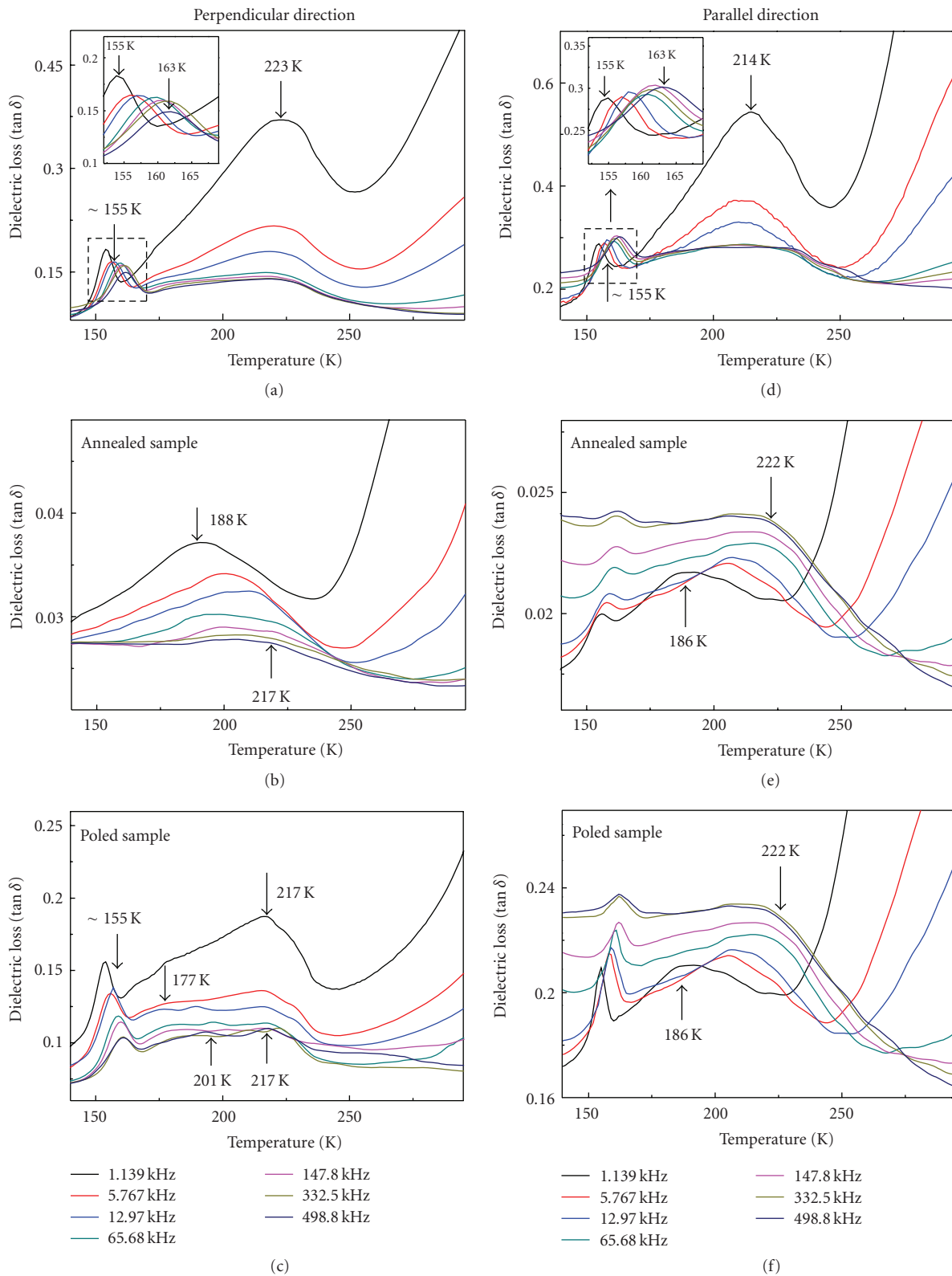


FIGURE 5: Dielectric Loss versus temperature for different frequencies: (a) perpendicular direction, inset: the enlarged ~ 155 K peak, (b) perpendicular direction by annealed, (c) perpendicular direction by poled, (d) parallel direction, inset: the enlarged ~ 155 K peak, (e) parallel direction by annealed, and (f) parallel direction by poled.

To get more information about the two dielectric loss peaks, the samples annealed in O₂ gas (5 mPa for 600°C/6 h) and poled in silicon oil at 180°C for 2 min under dc electric field of 20 kV/cm were measured. Figures 5(b), 5(e), 5(c), and 5(f) show the temperature dependence of dielectric loss ($\tan \delta$) at 1.139 ~ 498.8 KHz with different samples. The results of annealed samples in O₂ gas show that the peaks of ~155°C disappeared (in $[\perp]$ sample) and became very weak (in $[\parallel]$ samples) (shown in Figures 5(b) and 5(e)). Activation energy related to oxygen vacancy has been reported as 0.57–0.73 eV in BIT [9, 14], 1.9 eV in (Pb,La)TiO₃ [21], 0.97 in SrBi₂Ta₂O₉ [22], and 0.89–1.13 eV in SrTiO₃ [23]. Compared to these BIT results, our value of activation energy was higher. We tend to attribute such difference in activation energy to the fact that our corresponding temperature (155 K) used to estimate the activation energy is lower than that adopted in the literatures (500 K).

In the higher temperature, the thermodynamic energy and mobility of oxygen vacancies were higher, the activity energy was lower. So, we concluded that the peaks of ~155°C are related to V_O^\bullet , and the activity energy of this dielectric relaxation is 1.36 eV. The anomalies in ϵ - T curve at around 157 K are related to oxygen vacancies [24]. Still, the intensity of peaks in $[\parallel]$ sample was higher than in $[\perp]$ sample due to the effect of (Bi₂O₂)²⁺ layer. In Aurivillius compounds, the (Bi₂O₂)²⁺ layer serves as charge storage and insulating layer; the V_O^\bullet could not get across the (Bi₂O₂)²⁺ layer, therefore, the ~155°C peaks disappear or, not detected by dielectric measurement.

Also in Figures 5(b) and 5(e), we find again, in the $[\perp]$ sample, at about 188 K and 222 K, two dielectric anomalies appear and in the $[\parallel]$ sample, the peak of ~188 K shifts to higher temperature with the increase of the frequency. The phenomenon was similar to $\tan \delta$ - T curve of $[\perp]$ sample and $[\parallel]$ sample being poled. The dielectric loss versus temperature curve of $[\perp]$ sample and $[\parallel]$ sample by poled are shown in Figures 5(c) and 5(f). Compared to unpoled samples results, we clearly discovered that (1) the ~155 K peak was inconspicuously changed by poling treatment; (2) in the perpendicular direction sample, there appear two dielectric loss peaks in ~177 K and 217 K, the ~177 K peak shifts to higher temperature with the increase of the frequency, and the 217 K peak behaves asymmetrically in shape with the higher temperature side of the peak steeper than that of the lower side; (3) in the parallel direction sample, the dielectric loss peak shifts to higher temperature with the increase of the frequency and behaves as relaxation characteristic. By summarizing the above-mentioned results, we think that (1) the 223 K and 214 K peaks were combined with two dielectric loss peaks, the lower temperature peak (~190 K) relates to polarizable domains, and the higher temperature peak (~210 K) behaves asymmetrically in shape with the higher temperature side of the peak steeper than that of the lower side. A possible mechanism of the peak is the viscous motion of domain walls due to defect pinning and interaction of domain walls. Similar peaks were found in BIT, and a lot of ferroelectric and ferroelastic materials at lower T_c , [12, 13, 25, 26] are the possible mechanism of the dielectric anomalies at 232 K (shown in Figure 4);

(2) the disparity between the domain structures along the poling field is related to the different grain orientation of the samples being examined. Different domains have different sensibility of poling field, so that the poling effect along the c axis was greater than that along the a/b direction. Moreover, the polarization in BIT mainly comes from the contribution of a/b direction which might be responsible for the lower piezoelectric activity in BIT samples.

4. Conclusions

The grain-orientated BIT samples was prepared by the solid-state reaction method with several calcination process. The XRD patterns of all the parallel and perpendicular samples exhibit grain-oriented ceramics of the BIT samples. At the room temperature at frequencies of 1.139 kHz, the value of the dielectric constants with $[\perp]$ and $[\parallel]$ samples were about 91 and 195, respectively. The grain-oriented samples of BIT exhibit anisotropic properties with crystal structure, ferroelectric, piezoelectric, and dielectric properties, the $2P_r$ or d_{33} of \parallel and \perp samples were 49.5 $\mu\text{C cm}^{-2}$, 6.7 $\mu\text{C cm}^{-2}$ and 22.2 pC N⁻¹, 6.9 pC N⁻¹, respectively. Dielectric properties in temperature range of 140–300 K were investigated in two direction samples. Two dielectric anomalies were found at ~157 and ~223 K, respectively. The dielectric anomalies in around 157 K were related to oxygen vacancies. The activation energy of the dielectric relaxation of this process is estimated to be 1.36 eV. Another dielectric anomalies in around 232 K relates to polarizable domains and the viscous motion of domain walls.

Acknowledgment

This work was supported by the National Natural Science Foundation of China (Grant no. 51072177) and the Jiangsu Natural Science Foundation (Grant no. BK2005052).

References

- [1] E. C. Subbarao, "Ferroelectricity in Bi₄Ti₃O₁₂ and its solid solutions," *Physical Review*, vol. 122, no. 3, pp. 804–807, 1961.
- [2] S. E. Cummins and L. E. Cross, "Crystal symmetry, optical properties, and ferroelectric polarization of Bi₄Ti₃O₁₂ single crystals," *Applied Physics Letters*, vol. 10, no. 1, pp. 14–16, 1967.
- [3] A. Fouskova and L. E. Cross, "Dielectric properties of bismuth titanate," *Journal of Applied Physics*, vol. 41, no. 7, pp. 2834–2838, 1970.
- [4] S. E. Cummins and L. E. Cross, "Electrical and optical properties of ferroelectric Bi₄Ti₃O₁₂ single crystals," *Journal of Applied Physics*, vol. 39, no. 5, pp. 2268–2274, 1968.
- [5] Z. S. Macedo and A. C. Hernandez, "Laser sintering of Bi₄Ti₃O₁₂ ferroelectric ceramics," *Materials Letters*, vol. 55, no. 4, pp. 217–220, 2002.
- [6] M. Alexe, J. F. Scott, C. Curran, N. D. Zakharov, D. Hesse, and A. Pignolet, "Self-patterning nano-electrodes on ferroelectric thin films for gigabit memory applications," *Applied Physics Letters*, vol. 73, no. 11, pp. 1592–1594, 1998.
- [7] B. H. Park, B. S. Kang, S. D. Bu, T. W. Noh, J. Lee, and W. Jo, "Lanthanum-substituted bismuth titanate for use in

- non-volatile memories,” *Nature*, vol. 401, no. 6754, pp. 682–684, 1999.
- [8] Y. Kan, X. Jin, P. Wang, Y. Li, Y.-B. Cheng, and D. Yan, “Anisotropic grain growth of $\text{Bi}_4\text{Ti}_3\text{O}_{12}$ in molten salt fluxes,” *Materials Research Bulletin*, vol. 38, no. 4, pp. 567–576, 2003.
- [9] T. Takeuchi, T. Tani, and Y. Saito, “Piezoelectric properties of bismuth layer-structured ferroelectric ceramics with a preferred orientation processed by the reactive templated grain growth method,” *Japanese Journal of Applied Physics*, vol. 38, no. 9 B, pp. 5553–5556, 1999.
- [10] J. Hao, X. Wang, R. Chen, Z. Gui, and L. Li, “Preparation of textured bismuth titanate ceramics using spark plasma sintering,” *Journal of the American Ceramic Society*, vol. 87, no. 7, pp. 1404–1406, 2004.
- [11] W. Chen, Y. Hotta, T. Tamura, K. Miwa, and K. Watari, “Effect of suction force and starting powders on microstructure of $\text{Bi}_4\text{Ti}_3\text{O}_{12}$ ceramics prepared by magnetic alignment via slip casting,” *Scripta Materialia*, vol. 54, no. 12, pp. 2063–2068, 2006.
- [12] H. S. Shulman, D. Damjanovic, and N. Setter, “Niobium doping and dielectric anomalies in bismuth titanate,” *Journal of the American Ceramic Society*, vol. 83, no. 3, pp. 528–532, 2000.
- [13] X. Y. Mao, J. H. He, J. Zhu, and X. B. Chen, “Structural, ferroelectric, and dielectric properties of vanadium-doped $\text{Bi}_{4-x/3}\text{Ti}_{3-x}\text{V}_x\text{O}_{12}$,” *Journal of Applied Physics*, vol. 100, no. 4, Article ID 044104, 5 pages, 2006.
- [14] W. Li, K. Chen, Y. Yao, J. Zhu, and Y. Wang, “Correlation among oxygen vacancies in bismuth titanate ferroelectric ceramics,” *Applied Physics Letters*, vol. 85, no. 20, pp. 4717–4719, 2004.
- [15] J. Zhai and H. Chen, “Ferroelectric properties of $\text{Bi}_{3.25}\text{La}_{0.75}\text{Ti}_3\text{O}_{12}$ thin films grown on the highly oriented LaNiO_3 buffered Pt/Ti/SiO₂/Si substrates,” *Applied Physics Letters*, vol. 82, no. 3, pp. 442–444, 2003.
- [16] Z. Shen, J. Liu, J. Grins et al., “Effective grain alignment in $\text{Bi}_4\text{Ti}_3\text{O}_{12}$ ceramics by superplastic-deformation-induced directional dynamic ripening,” *Advanced Materials*, vol. 17, no. 6, pp. 676–680, 2005.
- [17] A. Garg, Z. H. Barber, M. Dawber, J. F. Scott, A. Snedden, and P. Lightfoot, “Orientation dependence of ferroelectric properties of pulsed-laser-ablated $\text{Bi}_{4-x}\text{Nd}_x\text{Ti}_3\text{O}_{12}$ films,” *Applied Physics Letters*, vol. 83, no. 12, pp. 2414–2416, 2003.
- [18] E. C. Subbarao, “A family of ferroelectric bismuth compounds,” *Journal of Physics and Chemistry of Solids*, vol. 23, no. 6, pp. 665–676, 1962.
- [19] E. Sawaguchi and L. E. Cross, “Dielectric behavior of $\text{Bi}_4\text{Ti}_3\text{O}_{12}$ at low temperature,” *Materials Research Bulletin*, vol. 5, no. 2, pp. 147–152, 1970.
- [20] K. R. Chakraborty, S. N. Achary, S. J. Patwe, P. S. R. Krishna, A. B. Shinde, and A. K. Tyagi, “Low temperature neutron diffraction studies on $\text{Bi}_4\text{Ti}_3\text{O}_{12}$,” *Ceramics International*, vol. 33, no. 4, pp. 601–604, 2007.
- [21] M. Kuwabara, K. Goda, and K. Oshima, “Coexistence of normal and diffuse ferroelectric-paraelectric phase transitions in $(\text{Pb},\text{La})\text{TiO}_3$ ceramics,” *Physical Review B*, vol. 42, no. 16, pp. 10012–10015, 1990.
- [22] Z.-Y. Wang and T.-G. Chen, “Evidence for the weak domain wall pinning due to oxygen vacancies in $\text{SrBi}_2\text{Ta}_2\text{O}_9$ from internal friction measurements,” *Physica Status Solidi A*, vol. 167, no. 1, pp. R3–R4, 1998.
- [23] A. E. Paladino, “Oxidation kinetics of single-crystal SrTiO_3 ,” *Journal of the American Ceramic Society*, vol. 48, no. 9, pp. 476–478, 1965.
- [24] N. Zhong and T. Shiosaki, “Dielectric behavior of $\text{Bi}_{3.25}\text{La}_{0.75}\text{Ti}_3\text{O}_{12}$ ferroelectric film,” *Journal of Applied Physics*, vol. 100, no. 3, Article ID 034107, 2006.
- [25] X. B. Chen, C. H. Li, Y. Ding et al., “Dielectric relaxation and internal friction related to the mobility of domain wall in PZT ferroelectrics,” *Physica Status Solidi A*, vol. 179, no. 2, pp. 455–461, 2000.
- [26] C. Wang, Q. F. Fang, Y. Shi, and Z. G. Zhu, “Internal friction study on oxygen vacancies and domain walls in $\text{Pb}(\text{Zr},\text{Ti})\text{O}_3$ ceramics,” *Materials Research Bulletin*, vol. 36, no. 15, pp. 2657–2665, 2001.



Hindawi

Submit your manuscripts at
<http://www.hindawi.com>

